Available online at www.sciencedirect.com
ScienceDirect
Trans. Nonferrous Met. Soc. China 24(2014) 2239−2243
Transactions of Nonferrous Metals Society of China
www.tnmsc.cn

Effects of Y addition on microstructure and properties of Al−Zr alloys

Yong-zhi ZHANG[1,2], Hai-yan GAO[1,2], Yu-fei WANG[1,2], Jun WANG[1,2], Bao-de SUN[1,2], Sun-wang GU[3], Wei-ren YOU[3]

1. Shanghai Key Laboratory of Advanced High-temperature Materials and Precision Forming, Shanghai Jiao Tong University, Shanghai 200240, China;
2. The State Key Laboratory of Metal Matrix Composites, Shanghai Jiao Tong University, Shanghai 200240, China;
3. Zhongtian Technology Corporation, Nantong 226009, China

Received 17 October 2013; accepted 23 April 2014

Abstract: Microstructure and properties of Al−0.30Zr and Al−0.30Zr−0.08Y (mass fraction, %) alloys were investigated by electrical conductivity measurements, microhardness tests, scanning electron microscopy (SEM) and transmission electron microscopy (TEM). Micron-sized primary Al_3Y phases form within grains and at grain boundaries simultaneously as product of eutectic reaction in as-cast Al−Zr−Y alloys. The addition of Y obviously accelerates the precipitation kinetics of Al_3Zr ($L1_2$) in Al−Zr−Y alloys. The Al−Zr−Y alloys exhibit greater electrical conductivity during aging due to formation of increased volume fractions of $Al_3(Zr,Y)$ precipitates. In ternary Al−Zr−Y alloys, spheroidal $L1_2$-structured $Al_3(Zr,Y)$ precipitates with increased number density and smaller mean radius were observed. The Al−0.30Zr−0.08Y alloys show improved recrystallization resistance compared with Al−0.30Zr alloys

Key words: Al−Zr−Y alloy; yttrium; heat treatment; recrystallization; microstructure; mechanical property

1 Introduction

Addition of a small amount of Zr can improve the recrystallization resistance of deformed aluminum alloys due to formation of metastable Al_3Zr precipitates with $L1_2$ structure [1]. The Al_3Zr dispersoids, precipitated from supersaturated Al−Zr solid solution during aging, are resistant to coarsening and can impede the evolution of subgrain during the hot deformation and homogenization [2]. The effectiveness of precipitates will depend on their distribution, size and spacing [3]. However, Zr is readily to segregate at the dendrites centers of aluminum alloys during solidification, which leads to heterogeneous distribution of Al_3Zr. The precipitates free region is prone to recrystallization. The homogenization treatment could not improve the distribution of precipitates and eliminate the precipitates free region [4]. Moreover, the precipitation of Al_3Zr ($L1_2$) is relatively slow due to slow diffusivity of Zr in α(Al).

Investigations have been carried out to accelerate precipitation kinetics and improve distribution of precipitates through multi-step annealing procedures [5] and alloying additions, such as Er [6], Yb [7] and Sc [8−10], among which the effect of Sc on precipitation behavior in Al−Zr was investigated extensively. The combined additions of Er and Zr improve the precipitation hardening of aluminum alloys [6]. There is a synergetic effect of Yb and Zr on the precipitation evolution of Al−Zr−Yb alloys, which results in a significant aging strengthening at elevated temperatures [7]. Alloys containing both Sc and Zr show promising strength and recrystallization resistance due to the formation of $Al_3(Sc_{1-x}Zr_x)$ precipitates [9,10]. However, high cost of scandium limited its commercial use. Thus cheaper yet more effective alternative elements are expected to find widespread use in commercial alloys. Y locates at the same main group as Sc, and the two elements show similar chemical properties. However, in published literatures, few researches were found to focus on the precipitation evolution of Al−Zr−Y alloys. In the present work, effect of yttrium on microstructure and recrystallization of Al−Zr was investigated to explore possibility of optimizing the properties of Al−Zr alloys.

Foundation item: Project (2012CB619505) supported by the Basic Research Program of China; Project (51274141) supported by the National Natural Science Foundation of China
Corresponding author: Hai-yan GAO; Tel: + 86-21-54742661; E-mail: gaohaiyan@sjtu.edu.cn
DOI: 10.1016/S1003-6326(14)63339-2

2 Experimental

The alloys under study were prepared through the ingot metallurgy route in the laboratory. Al−0.30Zr and Al−0.30Zr−0.08Y alloys were investigated (all compositions are in mass fraction of % unless otherwise noted). Alloys were melted in alumina crucibles at 800 °C in the open air, using 99.99 Al, Al−4.6Zr and/or Al−10Y master alloy. After thoroughly stirring, the melt was poured into a graphite mold. The ingots for observation were then aged at 500 °C for 1−16 h and water quenched after each aging treatment. The as-cast samples for cold-rolled were aged at 500 °C for 12 h and then cold-rolled to 82% reduction.

FEI NOVA NanoSEM 230 field-emission scanning electron microscope (SEM) was employed to observe the distribution of precipitates at 10 kV using backscattered imaging mode. To calculate number density of precipitates, the maximum depth below specimen surface where precipitates can be detected was calculated to be 0.66 μm by applying the Kanaya−Okayama equation in Ref. [11]. Precipitates size and number density were analyzed using Image pro software. At least 100 precipitates were measured for each mean radius of precipitates and at least 6 random SEM images were analyzed for each number density. The morphology and structure of precipitates were investigated using JEM 2100F transmission electron microscope (TEM) operated at 200 kV. TEM specimens were prepared through mechanical grinding to less than 80 μm. The specimens were thinned by twin-jet electro-polishing at 12 V in a 30% nitric acid and 70% methanol solution cooled to −30 °C.

Electrical conductivity and Vickers microhardness of the specimens were measured. Electrical conductivity measurements were performed at ambient temperature using an FD-102 eddy current conductivity tester. Five measurements were recorded for each reading. Vickers microhardness measurements were performed on polished samples using a load of 1.96 N and a dwell time of 10 s. At least 10 microhardness measurements were taken as the experimental data.

3 Results and discussion

3.1 As-cast microstructure

The micron-sized primary Al_3Y phases formed within grains and at grain boundaries as production of eutectic reaction in as-cast Al−0.30Zr−0.08Y, as shown in Fig. 1. The inset TEM micrograph of Al−0.30Zr−0.08Y in Fig. 1 illustrates primary Al_3Y at grain boundary. Energy dispersive spectroscopy (EDS) analysis shows that composition of the primary phases is 78.40% Al, 21.31% Y and 0.29% Zr in mole fraction, which indicates the Al_3Y stoichiometry and trace amount of Zr in the primary phases. However, the formation of primary phases indicates only a fraction of Y added to the alloys is available in the solid solution for precipitation. For the relatively low equilibrium partition coefficient (k_0≈0.02) [12], supersaturated Y atoms were expelled from the grain and accumulated at the advancing solid−liquid interface. When the Y concentration approaches the eutectic point, Al_3Y will form as divorced eutectic. A coupled eutectic reaction was not observed because of the low volume fraction of the Al_3Y phases in the Al−Al_3Y eutectic and the slow growth kinetics of the intermetallic phase. Similar phenomenon was observed in the Al−Sc [13] and Al−Er [14] system.

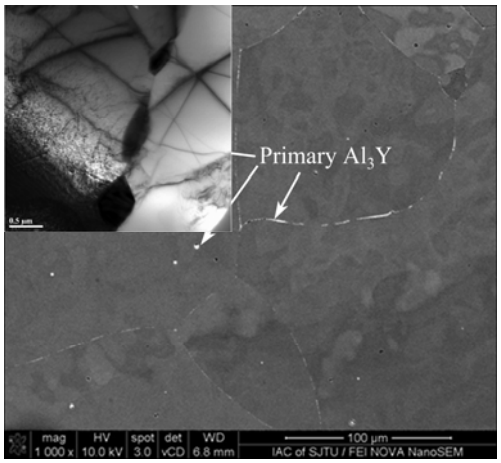

Fig. 1 SEM backscattered micrograph of as-cast Al−0.30Zr−0.08Y showing primary Al_3Y phases formed within grains and at grain boundaries during solidification (the inset bright-field TEM micrograph of as-cast Al−0.30Zr−0.08Y illustrates primary Al_3Y at the grain boundary)

3.2 Precipitation evolution during aging

Figure 2 illustrates precipitation behavior of Al−0.30Zr and Al−0.30Zr−0.08Y during aging as determined by electrical conductivity measurement. Al−Zr−Y exhibits relatively high electrical conductivity compared with Al−Zr during aging, indicating more alloy elements precipitated in ternary alloys. Investigations showed that influence of Zr in solid solution on electrical conductivity of aluminum alloys is approximately two orders of magnitude more than that in precipitation (0.17×10^{-8} Ω·m and 0.004×10^{-8} Ω·m per 0.1% Zr for solution elements and precipitation, respectively) [15]. By contrast, the similarity of as-cast electrical conductivities of Al−Zr and Al−Zr−Y alloys suggests that the effect of Y on the electrical conductivity is limited. Therefore, increase in conductivity during aging should mainly correspond to an increase of Zr in the form of precipitation and larger volume fraction of precipitates.

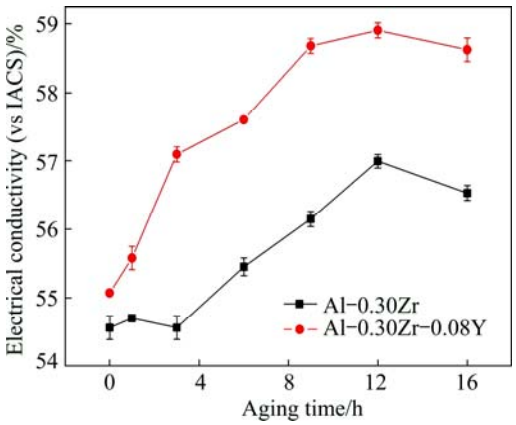

Fig. 2 Evolution of electrical conductivity during isothermal aging at 500 °C for Al−0.30Zr and Al−0.30Zr−0.08Y

The precipitation of Al_3Zr commences when the aging time is more than 3 h, as indicated by the increase in electrical conductivity in Al−Zr alloys, which suggests the slow precipitation kinetics due to the slow diffusivity for Zr in α(Al). The Al−0.30Zr alloy achieves a peak conductivity value of 57 % (vs IACS) which corresponds to a maximum volume fraction of Al_3Zr precipitates when aged for 12 h.

The rapid increase of electrical conductivity of Al−0.30Zr−0.08Y reveals that the precipitation commences when aging time is less than 1 h, indicating much faster precipitation kinetics in Al−Zr−Y alloys compared with Al−Zr. Coincided with Al−Zr alloys, Al−0.30Zr−0.08Y achieves peak electrical conductivity of 58.91% (vs IACS) when aged for 12 h. The change between as-cast and peak value in electrical conductivity of Al−0.30Zr−0.08Y alloys is 3.84% (vs IACS), which is larger than that of Al−0.30Zr (2.44% vs IACS), indicating that larger volume fraction of precipitates is generated in Al−Zr−Y. There is a decrease in electrical conductivity and hardness when the aging time is more than 12 h, which is due to coarsening and dissolution of $L1_2$-structured precipitates and their transformation to $D0_{23}$ structure, as reported in previous studies [1,2].

3.3 Distribution and structure of precipitates

Figure 3(a) and (b) show SEM images of nanoscaled precipitates in Al−0.30Zr and Al−0.30Zr−0.08Y aged at 500 °C for 12 h, respectively. It is apparent that compared with binary Al−0.30Zr alloys, precipitates with smaller radius and higher number density were obtained in Al−Zr−Y alloys. TEM observation revealed that the precipitates in both binary and ternary alloys kept spherical after aging for 12 h, as shown in Fig. 4. The

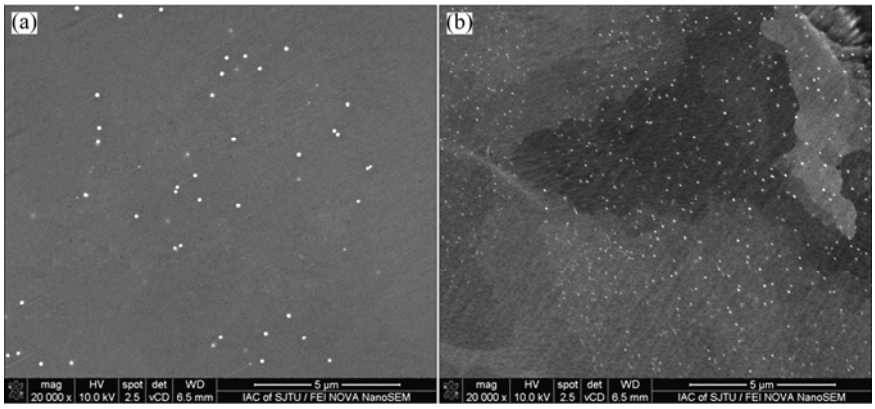

Fig. 3 SEM images of Al_3Zr and $Al_3(Zr,Y)$ precipitates in Al−0.30Zr (a) and Al−0.30Zr−0.08Y (b) aged at 500 °C for 12 h

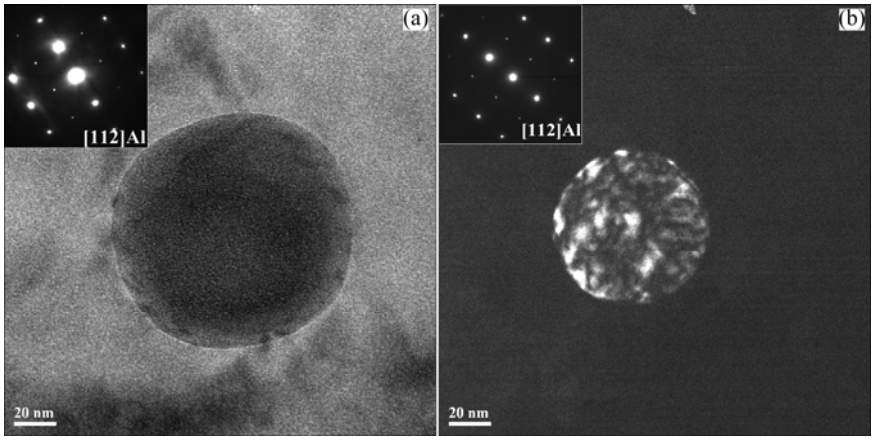

Fig. 4 Bright/dark field TEM micrographs of Al_3Zr and $Al_3(Zr,Y)$ precipitate in Al−0.30Zr (a) and Al−0.30Zr−0.08Y (b) aged at 500 °C for 12 h

superlattice diffraction points in selected area diffraction (SAD) in Figs. 4(a) and (b) indicate that the precipitates in Al−0.30Zr and Al−0.30Zr−0.08Y are both of the $L1_2$ structure. The composition of precipitates in Al−0.30Zr is determined by EDS to be 15.4% Zr and 84.6% Al. In contrast, the composition of precipitates in Al−0.30Zr−0.08Y is determined by EDS to be 8.40% Zr, 1.55% Y and 90.05% Al. Based on the results of SAD and EDS, it could be deduced that the precipitates in Al−0.30Zr and Al−0.30Zr−0.08Y are binary Al_3Zr and ternary $Al_3(Zr,Y)$ with $L1_2$ structure, respectively. The EDS results in Al−0.30Zr−0.08Y suggest that Zr is the dominant precipitating species, with Y partitioning weakly to the $Al_3(Zr,Y)$ precipitates.

The measured number density, average radius and volume fraction of precipitates in Al−Zr−(Y) alloys aged at 500 °C for 12 h are shown in Table 1. The number density of precipitates in Al−0.30Zr−0.08Y is nearly seven times that in Al−0.30Zr. The primary Al_3Y phases in Al−Zr−Y alloys reduce Y in the solid solution, which suggests that the effect of trace Y in α(Al) matrix on the increase of nucleation rates of precipitates is distinct. The smaller radius of precipitates in Al−Zr−Y alloys may result from the competition for available Zr solute between nucleation and growth [16]. At higher nucleation rate, more precipitates form, each of which is only able to grow to a smaller size before exhausting the supersaturated Zr. Volume fraction of precipitates in Al−Zr−Y is larger than that in Al−Zr, which is consistent with the electrical conductivity measurements.

Table 1 Average radius, r, number density, N, volume fraction, f, and Zener-drag, $P_Z \propto (f/r)$ of precipitates in Al−Zr−(Y) alloys aged at 500 °C for 12 h

Alloy	r/nm	N/m^{-3}	f/%	(f/r)/ 10^5 nm^{-1}
Al−0.30Zr	53.9±11.0	1.16×10^{18}	0.076	1.41
Al−0.30Zr−0.08Y	37.2±10.9	7.78×10^{18}	0.168	4.52

3.4 Recrystallization resistance

In order to investigate the recrystallization resistance of alloys, the cold-rolled samples were annealed at 350 °C for 120 min. Figure 5 shows the hardness−annealing time curves of the cold-rolled alloys at 350 °C. The hardness of Al−0.30Zr−0.08Y decreases more slowly than that of Al−0.30Zr. This indicates that the addition of Y improves the recrystallization resistance of cold-rolled Al−Zr alloys.

The Al_3Zr or $Al_3(Zr,Y)$ precipitates can exert a drag force (Zener-drag), P_Z, on the mobile subgrain boundaries, which prevents the subgrains from becoming potential nuclei for recrystallization [17]. A widely used relationship for the Zener-drag is $P_Z=3f\gamma_{GB}/2r$ [18], where γ_{GB} is the specific grain boundary energy, f is the volume fraction and r is the radius of precipitates. The equation illustrates that a higher (f/r)-ratio, i.e., a large volume fraction of small precipitates, should favor to attaining a large Zener-drag. The calculated f/r-ratios of precipitates are shown in Table 1, suggesting that the Zener-drag of $Al_3(Zr,Y)$ in Al−0.30Zr−0.08Y is three times that of Al_3Zr. Therefore, the $Al_3(Zr,Y)$ precipitates exert a high retarding force upon dislocation and grain boundaries, leading to improved recrystallization resistance of Al−Zr−Y alloys.

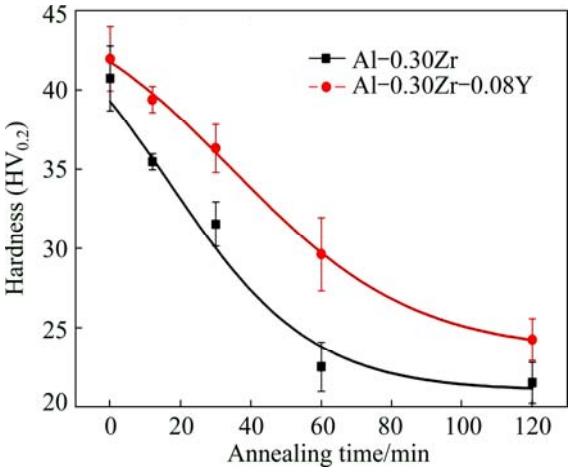

Fig. 5 Hardness as function of annealing time at 350 °C for cold-rolled Al−0.30Zr and Al−0.30Zr−0.08Y alloys

4 Conclusions

1) Micron-sized primary Al_3Y phases form within grains and at grain boundaries simultaneously as product of eutectic reaction in as-cast Al−Zr−Y alloys.

2) Addition of Y obviously accelerates the precipitation kinetics of precipitates in Al−Zr−Y alloys. The electrical conductivity of Al−Zr−Y is higher than that of Al−Zr during aging due to the precipitation of nanoscale $Al_3(Zr,Y)$ $(L1_2)$ precipitates with larger volume fraction.

3) $Al_3(Zr,Y)$ $(L1_2)$ precipitates with smaller radius and higher number density are obtained in Al−Zr−Y alloys.

4) The Al−0.30Zr−0.08Y alloys show improved recrystallization resistance compared with Al−0.30Zr alloys. It is consistent with the higher calculated Zener-drag of precipitates in Al−Zr−Y.

Acknowledgement

The authors thank Mr. Wei LI and Ms. Lin HE (Instrumental Analysis Center of Shanghai Jiao Tong University) for their help in SEM investigation.

References

[1] KNIPLING K E, DUNAND D C, SEIDMAN D N. Precipitation evolution in Al−Zr and Al−Zr−Ti alloys during isothermal aging at 375−425 °C [J]. Acta Materialia, 2008, 56: 114−127.

[2] KNIPLING K E, DUNAND D C, SEIDMAN D N. Precipitation evolution in Al−Zr and Al−Zr−Ti alloys during aging at 450−600 °C [J]. Acta Materialia, 2008, 56: 1182−1195.

[3] ROBSON J D, PRANGNELL P B. Modelling Al_3Zr dispersoid precipitation in multicomponent aluminium alloys [J]. Materials Science and Engineering A, 2002, 352: 240−250.

[4] KNIPLING K E, SEIDMAN D N, DUNAND D C. Ambient- and high-temperature mechanical properties of isochronally aged Al−0.06Sc, Al−0.06Zr and Al−0.06Sc−0.06Zr (at.%) alloys [J]. Acta Materialia, 2011, 59: 943−954.

[5] DENG Y L, WAN L, WU L H, ZHANG Y Y, ZHANG X M. Microstructural evolution of Al−Zn−Mg−Cu alloy during homogenization [J]. Journal of Materials Science, 2011, 46: 875−881.

[6] WEN S P, GAO K Y, LI Y, HUANG H, NIE Z R. Synergetic effect of Er and Zr on the precipitation hardening of Al−Er−Zr alloy [J]. Scripta Materialia, 2011, 65: 592−595.

[7] ZHANG Y Z, ZHOU W, GAO H Y, HAN Y F, WANG K, WANG J, SUN B D, GU S W, YOU W R. Precipitation evolution of Al−Zr−Yb alloys during isochronal aging [J]. Scripta Materialia, 2013, 69: 477−480.

[8] KNIPLING K E, KARNESKY R A, LEE C P, DUNAND D C, SEIDMAN D N. Precipitation evolution in Al−0.1Sc, Al−0.1Zr and Al−0.1Sc−0.1Zr (at.%) alloys during isochronal aging [J]. Acta Materialia, 2010, 58: 5184−5195.

[9] WANG Y, PAN Q L, SONG Y F, LI C, LI Z F, CHEN Q, YIN Z M. Recrystallization of Al−5.8Mg−Mn−Sc−Zr alloy [J]. Transactions of Nonferrous Metals Society of China, 2013, 23: 3235−3241.

[10] JIA Z H, ROYSET J, SOLBERG J K, LIU Q. Formation of precipitates and recrystallization resistance in Al−Sc−Zr alloys [J]. Transactions of Nonferrous Metals Society of China, 2012, 22: 1866−1871.

[11] GOLDSTEIN J I, NEWBURY D E, ECHLIN P, JOY D C, LYMAN C E, LIFSHIN E, SAWYER L, MICHAEL J R. Scanning electron microscopy and X-ray microanalysis [M]. New York: Plenum Press, 1994: 72−77.

[12] OKAMOTO H. Phase diagrams of dilute binary alloys [M]. Ohio: ASM International, 2002: 32−33.

[13] HYDE K B, NORMAN A F, PRANGNELL P B. The effect of cooling rate on the morphology of primary Al_3Sc intermetallic particles in Al−Sc alloys [J]. Acta Materialia, 2001, 49: 1327−1337.

[14] WEN S P, XING Z B, HUANG H, LI B L, WANG W, NIE Z R. The effect of erbium on the microstructure and mechanical properties of Al−Mg−Mn−Zr alloy [J]. Materials Science and Engineering A, 2009, 516: 42−49.

[15] MONDOLFO L F. Aluminum alloys: Structure and properties [M]. London: Butterworth, 1976: 82−85.

[16] ROBSON J D, PRANGNELL P B. Dispersoid precipitation and process modelling in zirconium containing commercial aluminium alloys [J]. Acta Materialia, 2001, 49: 599−613.

[17] FORBORD B, AURAN L, LEFEBVRE W, HALLEM H, MARTHINSEN K. Rapid precipitation of dispersoids during extrusion of an Al−0.91wt.%Mn−0.13wt.% Zr−0.17wt.% Sc-alloy [J]. Materials Science and Engineering A, 2006, 424: 174−180.

[18] NES E, RYUM N, HUNDERI O. On the Zener drag [J]. Acta Metallurgica, 1985, 33: 11−22.

Y 对 Al−Zr 合金微观组织与性能的影响

张永志[1,2]，高海燕[1,2]，王宇飞[1,2]，王 俊[1,2]，孙宝德[1,2]，顾孙望[3]，尤伟任[3]

1. 上海交通大学 上海市先进高温材料及其精密成形重点实验室，上海 200240；
2. 上海交通大学 金属基复合材料国家重点实验室，上海 200240；
3. 中天科技有限公司，南通 226009

摘 要：采用电导率、显微硬度、扫描电子显微镜(SEM)和透射电子显微镜(TEM)研究 Al−0.30Zr 与 Al−0.30Zr−0.08Y 合金的微观组织与性能。铸态 Al−Zr−Y 合金中微米尺度初生 Al_3Y 相通过共晶反应在晶内和晶界上同时生成。在 Al−Zr−Y 合金中，Y 明显加速了 $Al_3Zr(L1_2)$的析出动力学。由于较大体积 $Al_3(Zr,Y)$析出相的生成，Al−Zr−Y 合金的电导率明显高于 Al−Zr 合金的。在 Al−Zr−Y 合金中观察到了高密度的弥散球状 $L1_2$ 结构 $Al_3(Zr,Y)$析出相。Al−0.30Zr−0.08Y 合金具有比 Al−0.30Zr 合金更强的抗再结晶能力。

关键词：Al−Zr−Y 合金；钇；热处理；再结晶；微观组织；力学性能

(Edited by Hua YANG)